VNU Journal of Science: Mathematics - Physics
Journal homepage: https://js.vnu.edu.vn/MaP

Original Article

Design and Characteristics of a Wireless Non-enzyme Glucose Sensor Based on Resonant LC Passive Circuit

Nguyen Van Phu, Bui Van Anh, Pham Van Thanh*

VNU University of Science, 334 Nguyen Trai, Thanh Xuan, Hanoi, Vietnam

Received 17 May 2024
Revised 29 May 2024; Accepted 10 December 2024

Abstract: In this work we present a development of a reusable wireless non-enzyme glucose sensor based on the resonant inductor-capacitor (LC) passive circuit fabricated explicitly on a low-cost FR4 substrate. In our experiments, glucose/water solutions with varying concentrations have been utilized to evaluate the characteristics of the proposed structure. The obtained results showed that the fabricated sensor's effectiveness in accurately identifying glucose concentrations ranging from 0.1 mM to 100 mM. The sensor's sensitivities were estimated to be 9.595 MHz/mM, 0.7659 MHz/mM, and 0.2709 MHz/mM for 0.1 to 0.9 mM, 1 to 10 mM, and 10 to 100 mM glucose concentration ranges, respectively. The sensor's limit of detection (LOD) was calculated to be 0.105 mM for the glucose range from 0.1 to 0.9 mM. In particular, the sensitivity changes most significantly within the glucose concentration range of 0.1 to 0.9 mM, indicating that the sensor is particularly effective at detecting lower glucose concentrations. The obtained characteristics suggest that this sensor is suitable for applications requiring precise measurements of glucose solution.

Keywords: Radio frequency resonator, non-invasive glucose biosensor, quantitative detection, LC passive sensor, series resonance, wireless.

1. Introduction

Diabetes mellitus encompasses several conditions characterized by the body's impaired ability to process blood sugar (glucose), which is vital for energizing the muscle cells and tissues and serves as the primary fuel for the brain [1]. The primary causes of diabetes differ depending on the type. However, all forms of diabetes result in elevated blood sugar levels, which can cause significant health issues if not managed properly. Therefore, it is essential to devise a method that enables precise glucose detection

* Corresponding author.
E-mail address: phamvanthanh@hus.edu.vn

https//doi.org/10.25073/2588-1124/vnumap.4939

for the effective treatment and management of diabetes. Currently, invasive blood glucose detection technologies dominate the market due to their convenience and practicality, making them the preferred method for both hospital settings and household glucometers [2]. This method involves drawing a blood sample and then analyzing it *ex vivo* to measure the glucose concentration. In hospitals, blood is typically drawn from patients in the morning after an overnight fast and analyzed using automatic biochemical analyzers to ensure accurate results. While this approach provides precise measurements that are crucial for diagnosing diabetes, it is not suitable for continuous monitoring of diabetic patients. Nowadays, non-invasive blood glucose monitoring involves measuring blood glucose levels without harming human tissues, as suggested by the term. This technology encompasses a variety of detection methods, typically categorized into optical, microwave, electrochemical, and radio frequency (RF) techniques. Among these techniques, a biosensor for glucose detection that utilizing RF techniques has garnered significant interest and is considered a strong and promising contender for the development of third-generation glucose biosensors [3-5]. RF biosensors present several benefits over other biosensor types [6]. Firstly, they differ from electrochemical biosensors, which are limited by environmental conditions and tend to degrade over time. RF biosensors are immune to environmental influences such as external light, temperature, and humidity, ensuring stable performance in complex, long-term settings. Secondly, RF biosensors can rapidly detect biomarkers in real-time, eliminating the need for any pre-stabilization period. Thirdly, detection speed with RF biosensors depends only on the sweep period of the vector network analyzer, which means they can provide results much faster. Finally, RF biosensors allow for label-free detection; they do not require the addition of special markers for sensing, as the substance to be tested is placed directly in the sensor's detection zone. This facilitates a more straightforward and efficient detection process [7]. Especially there have been several studies using a wireless resonant LC passive circuit for sensing glucose concentrations and providing highly reliable results that can be integrated into tags [8-10]. The diagram of the wireless LC passive sensor is shown in Fig. 1

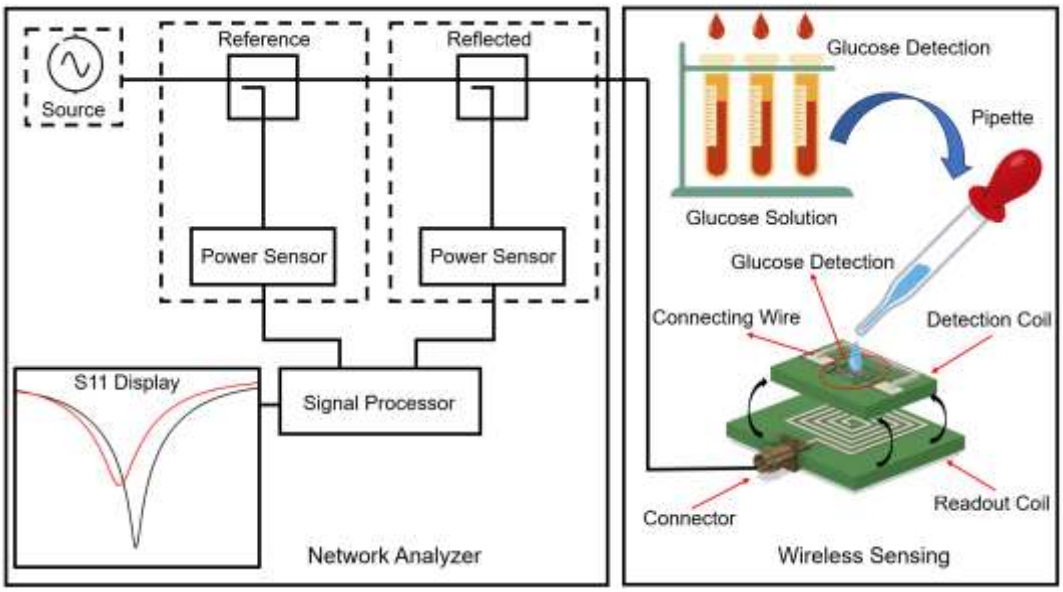

Figure 1. The working principle diagram of the wireless LC passive sensor.

In this work, a wireless LC passive non-enzyme glucose sensor has been developed. This sensor incorporates specially designed interdigitated electrode (IDE) capacitors, essential to its functionality. A significant finding from the study is that glucose concentrations show a direct correlation with the

resonance frequency of the LC passive circuit. This relationship indicates that changes in either parameter can be precisely utilized to determine different glucose levels, thus confirming the sensor's ability to monitor glucose accurately. These results underscore the practical utility of this innovative sensor in continuous glucose monitoring and suggest its potential to transform the field of non-invasive glucose testing. The design of this sensor leverages capacitors made using printed circuit board (PCB) technology, which accelerates the fabrication process and reduces costs compared to other glucose sensing methods. Besides, this study highlights the advantages of non-enzymatic sensing. Unlike traditional glucose sensors that rely on enzymatic reactions, which can degrade over time affecting sensor stability and lifespan, a non-enzymatic sensor utilizing a resonant LC passive circuit is not subject to enzyme-related degradation. This key feature significantly enhances the sensor's durability and reliability, making it an attractive option for long-term glucose monitoring. Moreover, the wireless nature of this sensor enhances its integration into wearable devices, enabling continuous, real-time monitoring without the need for direct physical connections. This feature can significantly boost patient compliance and comfort by allowing users to monitor their glucose levels more discreetly and conveniently, thus encouraging more consistent use and better management of their condition.

2. Working Principle and Sensor Design

2.1. Working Principle of a Wireless Resonant LC Passive Sensor

The suggested design utilizes a mix of interdigitated electrode capacitors and LC passive sensing methods for contact glucose detection. This approach relies on measuring shifts in the resonant frequency of the LC passive circuit. This wireless LC passive sensor operates through the mutual inductance coupling between the primary and secondary inductors. This coupling allows the sensor to identify changes in environmental conditions or the properties of objects by monitoring fluctuations in the mutual inductances, as illustrated in Fig. 1.

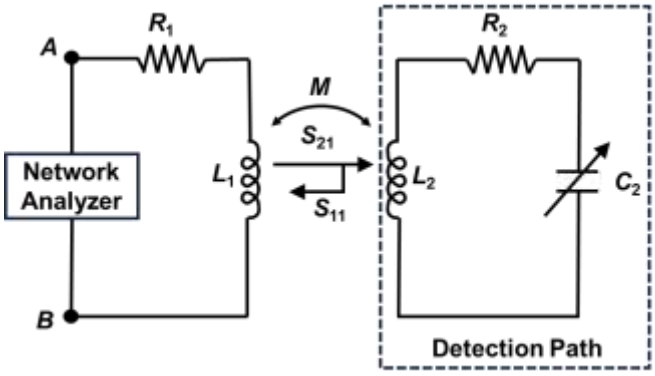

Figure 2. Circuit diagram of the passive LC wireless sensor.

Figure 2 shows the circuit diagram of the sensor. The primary inductor L_1 is wireless magnetically linked with the secondary inductor L_2. As the energy transmitter, the primary inductor L_1 dispatches power to the secondary inductor L_2, which acts as the signal receiver. This setup reflects the resonance frequency of the LC sensing circuit, which is constituted by the detection pathway involving inductor L_2 and the sensing capacitor C_2. This configuration allows precise monitoring and analysis of resonance frequency changes, enhancing the sensor's responsiveness and accuracy in detecting environmental

variations. R_1 and R_2 represent the parasitic resistances associated with the respective inductors in this configuration. The input impedance Z_i, defined as the total impedance between points A and B, results from the combined impedances of the reader path Z_R and the detection path Z_d. This relationship is formalized in Eq. (1). The impedance model facilitates the analysis of how energy is transmitted and received within the system, impacting the overall sensitivity and accuracy of the sensor [11, 12].

$$Z_i = Z_R + Z_d = R_1 + j\omega L_1 + \frac{(\omega M)^2}{R_2 + j\omega L_2 - j\left(\frac{1}{\omega C_2}\right)} \quad (1)$$

In Eq. (1), ω represents the angular frequency (rad/s), and M denotes the mutual inductance (H), R_1 and R_2 are series resistors (Ω) of coils. As illustrated in Equation 1, Z_i depends on the frequency, mutual inductance, and sensing capacitance. A periodic sweeping of frequency around the sensor's natural frequency is utilized to accurately track frequency variations rather than measuring the voltage change at a specific frequency. This method ensures more precise detection of resonance frequency shifts. Additionally, the mutual inductance, influenced by factors such as the setup's geometry, the distance between the coils (d), and the magnetic permeability of the inductance coil, plays a crucial role in determining the input impedance. Notably, with a constant geometry, the mutual inductance M decreases as the coupling distance d increases, which in turn affects the sensor's performance and sensitivity [11, 12]. Theoretically, the resonance frequency f_{res} of the detection path and the quality factor Q can be described by the following expressions [13]:

$$f_{res} = \frac{1}{2\pi\sqrt{L_2 C_2}} \quad (2)$$

$$Q = \frac{1}{R_2} \times \sqrt{\frac{L_2}{C_2}} \quad (3)$$

An alternating signal with a frequency sweep is applied to the primary inductor L_1, which transmits electromagnetic energy to the detection path via the secondary inductor L_2. Within this frequency sweep, when the frequency reaches the point corresponding to the resonance frequency of the detection path, there will be a significant alteration in the input impedance of the primary inductor L_1. This change in impedance affects the input reflection coefficient S_{11}, which quantifies the ratio of reflected power to incident power. Any alterations in the dielectric medium between the electrodes can lead to variations in capacitance C_2, prompting a shift in the LC circuit's resonance frequency, which is determined by the minimum point of the S_{11} parameter. This shift in resonance frequency can be thoroughly investigated and identified by analyzing the changes in the reflection coefficient S_{11} on L_1 measured by the network analyzer device. This method allows precise monitoring and detection of environmental changes or material characteristics within the sensor's proximity. The sensing capacitor can be constructed using a capacitively coupled contact electrode structure, which allows it to leverage the benefits outlined earlier. The proposed structure employs frequency shift measurement techniques to enhance performance. It achieves precise measurements by translating environmental changes between the sensing electrodes into the device's resonance frequency shifts. In this work, the LC passive sensing structure was adopted and integrated with a uniquely designed IDE capacitor structure. This approach, which combines traditional techniques with advanced structural design, is employed to enhance the capabilities and effectiveness of the sensor. To construct a sensing system, the sensing inductor was serially connected to an IDE capacitor structure. As previously mentioned, alterations in the dielectric medium between the electrodes of the IDE capacitor result in changes in capacitance, which, in turn, lead to variations in the resonance frequency of the LC circuit

2.2. Sensor Design

The sensor's structure introduced in this research includes a planar square spiral inductor (L_2) connecting with an IDE capacitor that acts as the sensing element. While another planar square spiral inductor is used as a read-out antenna (L_1) for S_{11} measurement. Figure 3 shows the structure of the proposed LC passive wireless sensor.

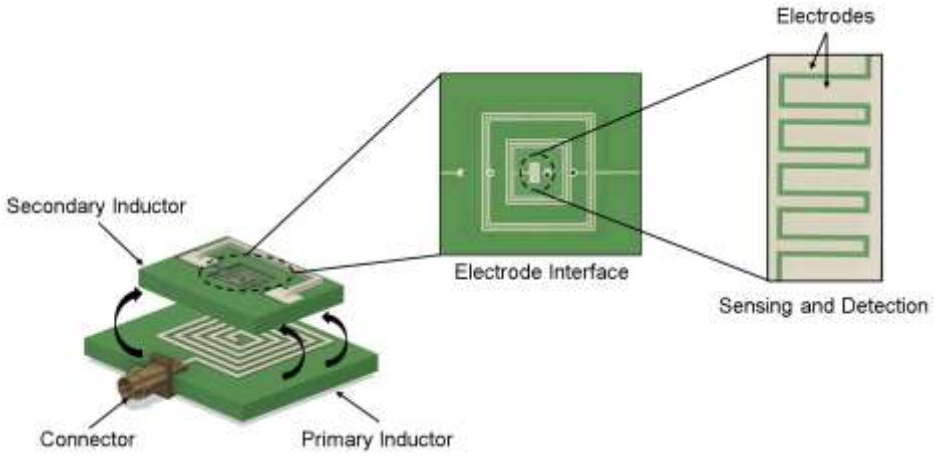

Figure 3. Design of a non-enzyme glucose sensor based on the wireless LC passive circuit.

The sensing system includes two copper electrodes wrapped around the interface of the printed circuit board (PCB) and two inductors designated for transmitting and receiving radiation. These inductors are positioned separately with air space between them of 2.0 mm. An IDE capacitor was incorporated between two sections of a square-shaped spiral inductor L_2, creating a compact resonator LC passive tank. The gap between the sensor electrodes in the IDE was initially set at 0.1 mm.

3. Experiment

3.1. LC Passive Circuit Fabrication

Fabrication process of these devices is combined with the advanced 3D printing technology with standard printed circuit board (PCB) techniques. This innovative approach offers several advantages over traditional fabrication methods, including cost-effectiveness, simplicity, and notably faster production times. In this work, the microelectrode structure was intricately patterned onto commercial copper-FR4 substrates and then coated with a layer of tin (Sn) plating, all achieved through precise PCB methodologies. Figure 4a shows the primary inductor used as a read-out antenna L_1. This coil is a planar spiral square antenna with 5 turns; its turn width is 1.0 mm, the spacing between turns is 1.0 mm, and the outer diameter is 21.0 mm; therefore, the inductance of this antenna is calculated to be 0.61 μH. Figure 4b shows the resonant LC passive circuit, including a coil L_2 connected with an IDE capacitor. The L_2 is a planar spiral rectangular coil with 10 turns; its length and width are 7.9 mm and 6.3 mm, its turn width is 0.1 mm; the designed spacing between turns is 0.1 mm, and the inductance of the L_2 coil is calculated to be 0.43 μH. The IDE capacitor is designed with an area of 1.5 x 1.9 mm with 10 fingers, as illustrated in Figure 4b.

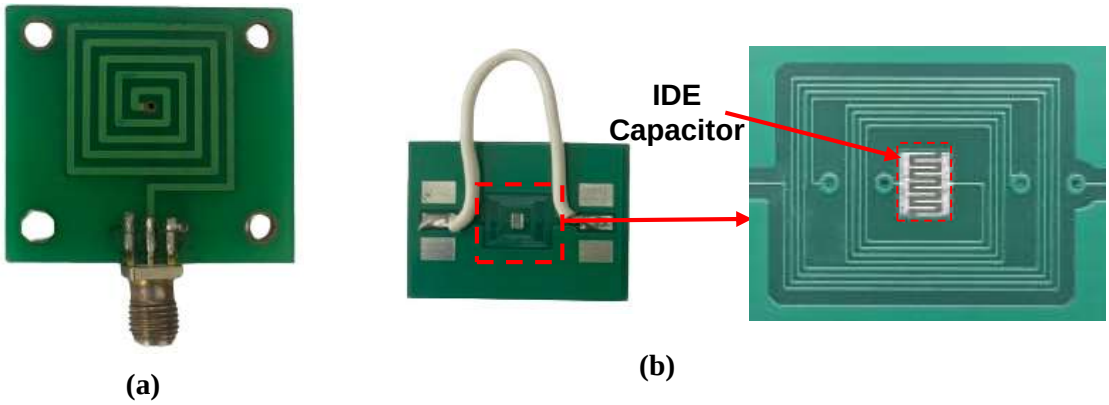

Figure 4. Practical LC wireless passive sensor structure. (a) The fabricated L1 antenna. (b) The fabricated resonant LC passive circuit.

3.2. Preparation of Glucose Solution

The solutions utilized for experiments were of deionized water (DI) combined with glucose powder purchased from Sigma-Aldrich (St. Louis, MO, USA). Different electrical properties, including electrical conductivity and electrical permeability were studied. This work involved preparing mixtures with concentrations ranging from 0.1 to 0.9 mM, 1 to 9 mM, and 10 to 100 mM. All samples were prepared at 25 °C and stored between 0-4 °C until measurements.

3.3. Experiment Setup for Glucose Concentration Measurement

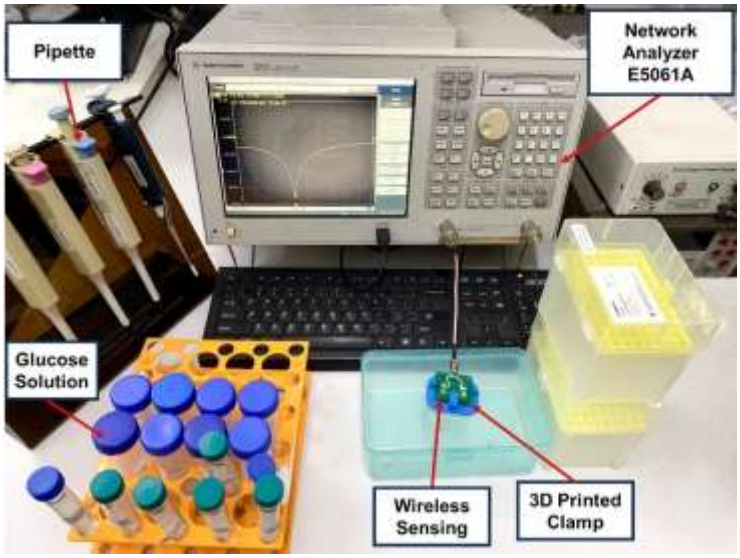

Figure 5. Experimental setup.

The experimental setup depicted in Figure 5 was meticulously organized to ensure precise measurements. An ENA series network analyzer (Agilent E5061A ENA Series) measured the reflection coefficient S_{11} across a range of sweeping frequencies, allowing for detailed analysis. The LC passive sensor and a critical componentwere efficiently developed using rapid prototyping techniques, which involved a meticulously designed 3D-printed mold, ensuring high precision and consistency in the sensor's fabrication. Additionally, glucose solution was applied directly onto the IDE capacitor position of the sensor using a pipette, ensuring be controlled for the precision application.

4. Results and Discussion

To evaluate the change of the resonant frequency on the conductivity of the solution filled in the IDE capacitor, the glucose solution with different concentrations ranging from 1 mM to 100 mM was prepared and injected into the IDE sensing area. The reflection coefficient S_{11} was measured, and the resonant frequency of the sensing resonant structure was derived by extracting the frequency value in whose reflection coefficient S_{11} achieves minima attenuation. Figure 6a illustrates the variation in resonance frequency as the chip undergoes filling with different concentrations of glucose, ranging from 0.1 mM to 0.9 mM. Besides, the dependence of the resonance frequency and reflection coefficient S_{11} on the concentration of Glucose is shown in Figure 6b. Figure 6a presents the internal normalized reflectivity measurement, highlighting the frequency range of 600 MHz to 700 MHz, indicating glucose's presence on the sensor electrode surface. Figure 6a details the gradual decrease in resonance frequency with increasing glucose concentration. Specifically, the experimental results show that as glucose concentration increases from 0.1 mM to 0.9 mM, the resonance frequency of the detection path decreases from 645.46 MHz to 637.89 MHz.

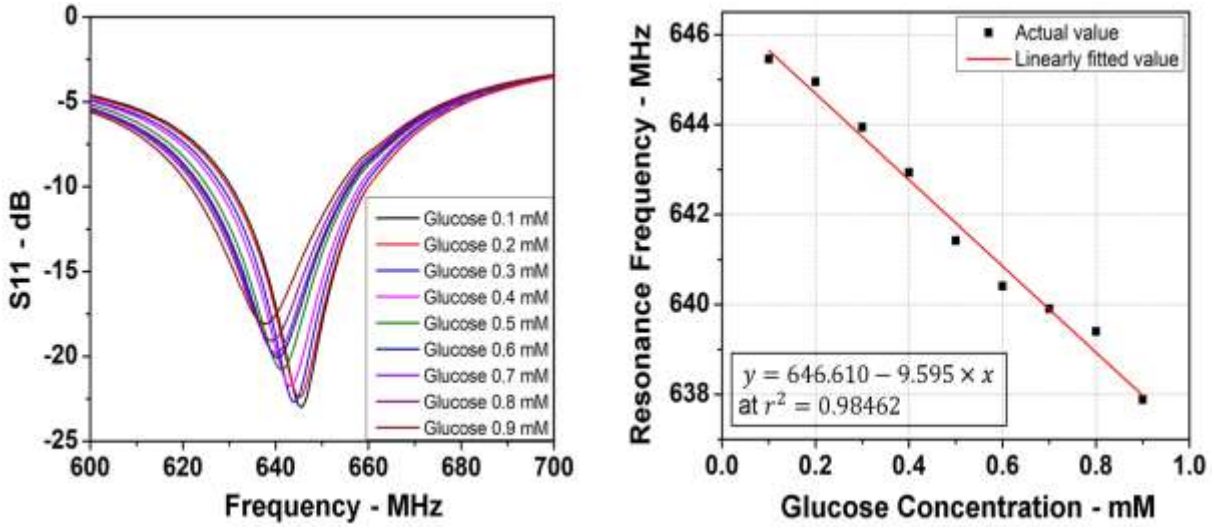

(a) (b)

Figure 6. a) The dependence of the reflection coefficient S_{11} on excitation frequency was examined for glucose concentrations from 0.1 mM to 0.9 mM (b) Regression analysis assessed the shift in resonance frequency and the magnitude of S_{11}.

The shift in the resonant frequency and changes in the measured S_{11} parameters result from the interaction between the resonator's inductor and capacitor and the glucose solution under test, influenced by the glucose permittivity. The sensor's resonant frequency experienced the most significant downward shift when the glucose concentration was decreased; this behavior is similar to other research [10, 14]. The regression analysis shows a strong linear correlation ($r^2 = 0.98462$) between glucose concentration and the shift in resonant frequency, with the linear regression equation expressed as follows:

$$Y_1\ [MHz] = 646.610 - 9.595 \times X\ [mM] \quad (4)$$

Here, Y represents the resonant frequency of the fabricated sensor, and X represents the glucose concentration. Consequently, the sensor demonstrated a sensitivity of 9.595 MHz/mM.

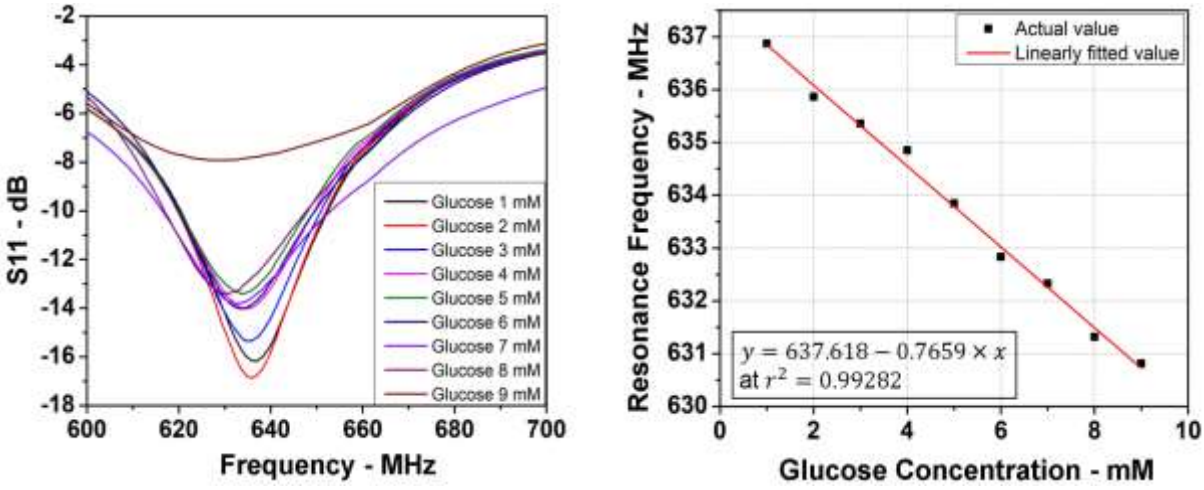

(a) (b)

Figure 7. (a) The relationship between the reflection coefficient S_{11} and excitation frequency was analyzed for glucose concentrations ranging from 1.0 mM to 9.0 mM (b) Regression analysis evaluated the shift in resonance frequency and the magnitude of S_{11}.

The change in resonance frequency was examined for glucose solution with concentrations ranging from 1 mM to 9 mM. The reflection coefficient S_{11} was measured, and the sensor's resonant frequency was determined by identifying the frequency at which the reflection coefficient S_{11} reached its minimum attenuation. Figure 7 illustrates the variation in resonance frequency as the sensor is filled with different glucose concentrations. Experimental results specifically demonstrate that as glucose concentration increases from 1.0 mM to 9.0 mM, the resonance frequency of the detection line decreases from 636.875 MHz to 630.815 MHz. The resonator frequencies experienced the most significant downward shift at the highest glucose concentration. Regression analysis reveals a strong linear correlation ($r^2 = 0.98462$) between glucose concentration and the change in the resonant frequency of the fabricated sensor, with the linear regression equation presented as follows:

$$Y_2\ [MHz] = 637.618 - 0.7659 \times X\ [mM] \quad (5)$$

Equation 6 indicates that the sensor exhibited a sensitivity of 0.7659 MHz/mM.

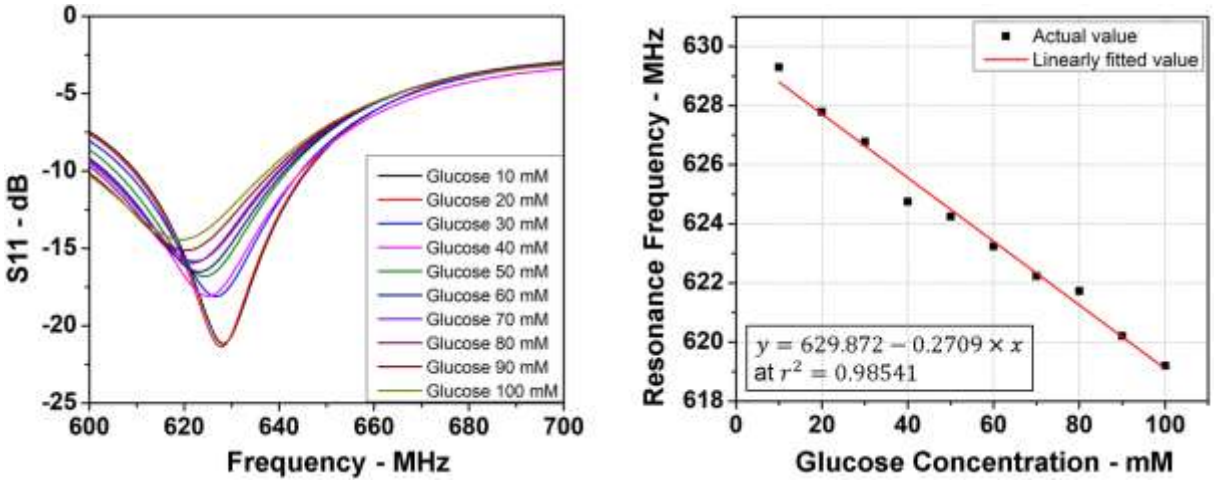

(a) *(b)*

Figure 8. (a) The analysis examined the relationship between the reflection coefficient S_{11} and excitation frequency for glucose concentrations varying from 10 mM to 100 mM (b) A regression analysis assessed the shift in resonance frequency and the changes in the magnitude of S_{11}.

Finally, the change in resonance frequency was examined based on the conductivity of glucose solutions contained in the IDE capacitor, with concentrations ranging from 10 mM to 100 mM. Figure 8 illustrates the variation in resonance frequency as the chip is filled with different glucose concentrations. This analysis reveals that as the glucose concentration increases, there is a notable shift in the resonance frequency and a corresponding change in the reflection coefficient S_{11}, underscoring the sensor's sensitivity to varying glucose levels. Experimental results specifically demonstrate that as glucose concentration increases from 10 mM to 100 mM, the resonance frequency of the detection line decreases from 629.3 MHz to 619.2 MHz. It was observed that higher glucose concentrations caused the resonance frequency to shift further towards a lower frequency. Moreover, the interaction between the resonator's inductor and capacitor with the tested material, influenced by the glucose solution's permittivity, results in changing of the resonant frequency and measured S_{11}-parameters. Among the materials tested, the 1 mM glucose solution caused the most significant downward shift in the resonant frequency due to its lower viscosity. Consequently, the resonator's resonant frequency experienced a downward shift at the lower glucose concentration. This outcome was expected, given that the dielectric constant of glucose decreases as its concentration increases. Regression analysis reveals a strong linear correlation ($r^2 = 0.98541$) between glucose concentration and the shift in resonant frequency, with the linear regression equation as follows:

$$Y_3\ [MHz] = 629.872 - 0.2709 \times X\ [mM] \quad (6)$$

Equation 7 indicates that the sensor exhibited a sensitivity of 0.2709 MHz/mM. Notably, a strong linear correlation exists between glucose concentration and resonance frequency.

From Eqs (5), (6) and (7), it is evident that each concentration region yields different sensitivities, and the sensitivity tends to decrease as glucose concentration increases. The sensitivity changes most significantly when the glucose concentration ranges from 0.1 to 0.9 mM, and the limit of detection (LOD) of the sensor in this range is calculated to be 0.105 mM using the formula of 3σ/m, where σ is the standard deviation of blank solution and m is the slope of the linear regression [15]. These obtained

parameters of the fabricated sensor suggest that it is particularly effective in detecting lower glucose concentrations, making it suitable for applications requiring precise measurement in this concentration range.

5. Conclusion

In this work, an integrated LC passive biosensor for glucose concentration measurement based on a frequency resonator was successfully fabricated on commercial FR4 substrates. Experimental results showed that the resonant frequency of the sensor resonator decreases when the glucose concentration increases from 0.1 mM to 100 mM. Notably, the sensor's sensitivity differed in different concentration regions, with a general trend of decreasing sensitivity as glucose concentration increased. The sensor's sensitivities were estimated to be 9.595 MHz/mM, 0.7659 MHz/mM, and 0.2709 MHz/mM for 0.1 to 0.9 mM, 1 to 10 mM, and 10 to 100 mM glucose concentration ranges, respectively. The sensor's limit of detection (LOD) was calculated to be of 0.105 mM for the glucose range from 0.1 to 0.9 mM. In particular, the concentration changes most significantly in the glucose concentration range located at 0.1 mM to 0.9 mM. The results demonstrate that the proposed resonant sensor structure is effective and suitable for precision measurements within this concentration range. The study highlights the potential of the wireless non-enzyme glucose sensor based on a resonant LC passive circuit as a significant innovation in biomedical device technology for glucose monitoring. Due to utilizing a non-enzymatic approach, this sensor offers advantages in terms of stability and durability compared to traditional enzyme-based glucose sensors. Its versatility also paves the way for new possibilities in advanced diagnostics and health monitoring.

Acknowledgments

This research is funded by Vietnam National Foundation for Science and Technology Development (NAFOSTED) under grant number 103.99-2020.33. Phu Nguyen Van was funded by the Master, Ph.D. Scholarship Programme of Vingroup Innovation Foundation (VINIF), code VINIF.2023.ThS.105.

References

[1] K. S. Leong, J. P. Wilding, Obesity and Diabetes, Best Pract. Res. Clin. Endocrinol. Metab., Vol. 13, No. 2, 1999, pp. 221-237, https//doi.org/10.1053/beem.1999.0017.

[2] W. Villena Gonzales, A. Mobashsher, A. Abbosh, The Progress of Glucose Monitoring-A Review of Invasive to Minimally and Non-Invasive Techniques, Devices and Sensors, Sensors, Vol. 19, No. 4, 2019, pp. 800, https//doi.org/10.3390/s19040800.

[3] C. Jang, H. J. Lee, J. G. Yook, Radio-Frequency Biosensors for Real-Time and Continuous Glucose Detection, Sensors, Vol. 21, No. 5, 2021, pp. 1843, https//doi.org/10.3390/s21051843.

[4] Y. Li, Z. Yao, W. Yue, C. Zhang, S. Gao, C. Wang, Reusable, Non-Invasive, and Ultrafast Radio Frequency Biosensor Based on Optimized Integrated Passive Device Fabrication Process for Quantitative Detection of Glucose Levels, Sensors, Vol. 20, No. 6, 2020, pp. 1565, https//doi.org/10.3390/s20061565.

[5] H. Zafar, A. Channa, V. Jeoti, G. M. Stojanović, Comprehensive Review on Wearable Sweat-Glucose Sensors for Continuous Glucose Monitoring, Sensors, Vol. 22, No. 2, 2022, pp. 638, https//doi.org/10.3390/s22020638.

[6] N. Y. Kim, K. K. Adhikari, R. Dhakal, Z. Chuluunbaatar, C. Wang, E. S. Kim, Rapid, Sensitive, Reusable Detection of Glucose by A Robust Radiofrequency Integrated Passive Device Biosensor Chip, Sci. Rep., Vol. 5, 2015, pp. 1-9, https//doi.org/10.1038/srep07807.

[7] L. Johnston, G. Wang, K. Hu, C. Qian, G. Liu, Advances in Biosensors for Continuous Glucose Monitoring Towards Wearables, Front. Bioeng. Biotechnol., Vol. 9, 2021, https//doi.org/10.3389/fbioe.2021.733810.

[8] V. Turgul, I. Kale, Permittivity Extraction of Glucose Solutions Through Artificial Neural Networks and Non-Invasive Microwave Glucose Sensing, Sensors Actuators, A Phys., Vol. 277, 2018, pp. 65-72, https//doi.org/10.1016/j.sna.2018.03.041.

[9] M. Dautta, M. Alshetaiwi, J. Escobar, P. Tseng, Passive and Wireless, Implantable Glucose Sensing with Phenylboronic Acid Hydrogel-Interlayer RF resonators, Biosens. Bioelectron., Vol. 151, 2020, pp. 112004, https//doi.org/10.1016/j.bios.2020.112004.

[10] H. Li, H. Xu, S. Lin, Y. Jia, A Wireless Resonant LC Sensor for Glucose Detection †, Eng. Proc., Vol. 27, No. 1, 2022, pp. 2-6, https//doi.org/10.3390/ecsa-9-13365.

[11] R. J. Rodrigues, A Experimental Method to the Study of Wireless Passive LC Sensors, Int. J. Biosens. Bioelectron., Vol. 4, No. 4, 2018, pp. 175-177, https//doi.org/10.15406/ijbsbe.2018.04.00121.

[12] Y. Wang, Y. Jia, Q. Chen, Y. Wang, A Passive Wireless Temperature Sensor for Harsh Environment Applications, Sensors, Vol. 8, No. 12, 2008, pp. 7982-7995, https//doi.org/10.3390/s8127982.

[13] L. D. Quang, T. T. Bui, A. B. Hoang, T. P. Van, C. P. Jen, T. C. Duc, Development of a Passive Capacitively Coupled Contactless Conductivity Detection (PC4D) Sensor System for Fluidic Channel Analysis Toward Point-of-Care Applications, IEEE Sens. J., Vol. 19, No. 15, 2019, pp. 6371-6380, https//doi.org/10.1109/JSEN.2019.2908179.

[14] A. E. Omer et al., Low-cost Portable Microwave Sensor for Non-Invasive Monitoring of Blood Glucose Level: Novel Design Utilizing A Four-Cell CSRR Hexagonal Configuration, Sci. Rep., Vol. 10, No. 1, 2020, pp. 15200, https//doi.org/10.1038/s41598-020-72114-3.

[15] M. F. A. M. Yunos et al., RF Remote Blood Glucose Sensor and a Microfluidic Vascular Phantom for Sensor Validation, Biosensors, Vol. 11, No. 12, 2021, pp. 494, https//doi.org/10.3390/bios11120494.